

# Revealing a Size-Resolved Fluorescence-Based Metric for Tracking Oxidative Treatment of Total *N*-Nitrosamine Precursors in Waters from Wastewater Treatment Plants

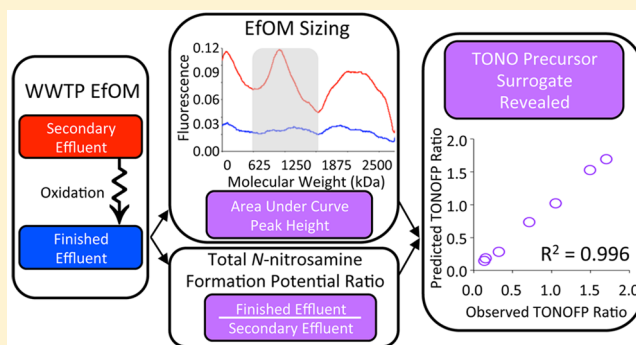
Erin M. Needham,<sup>†</sup> Adrian Fernandez de Luis,<sup>‡</sup> Justin R. Chimka,<sup>‡</sup> and Julian L. Fairey<sup>\*,†</sup>

<sup>†</sup>Department of Civil Engineering, University of Arkansas, Fayetteville, Arkansas 72701, United States

<sup>‡</sup>Department of Industrial Engineering, University of Arkansas, Fayetteville, Arkansas 72701, United States

## Supporting Information

**ABSTRACT:** *N*-Nitrosamines make up a nonhalogenated group of disinfection byproducts that form during chloramination, particularly in drinking waters impacted by wastewater treatment plant (WWTP) effluents. Here, we reveal a size-resolved fluorescence-based precursor surrogate for tracking total *N*-nitrosamine formation potential (TONOFP) through oxidative treatment. Samples were collected at seven WWTPs, at the finished effluent and prior to final disinfection (i.e., secondary effluent). Asymmetric flow field-flow fractionation (AF4) with inline fluorescence detection at excitation and emission wavelengths of 280 and 340 nm, respectively (i.e.,  $I_{280/340}$ ), showed protein-rich natural organic matter peaks between 10–445 and 445–1500 kDa. TONOFP was measured by chemiluminescence on samples dosed with 250 mg L<sup>-1</sup> Cl<sub>2</sub> monochloramine at pH 7 for 7 days. Metrics from AF4  $I_{280/340}$  (i.e., area under the curve and peak height) and  $I_{257/277}$  from whole water excitation–emission matrices were leveraged in multivariate models to develop correlations with TONOFP. The TONOFP of the finished effluent divided by that of the secondary effluent (i.e., the TONOFP Ratio) was strongly correlated ( $R^2 = 0.996$ ;  $p = 0.000$ ) to a model of AUC for the 10–445 kDa peak, maximal peak height, and  $I_{257/277}$ . This TONOFP precursor surrogate requires 2 mL of sample and is transformational with respect to assessing the impact of oxidative treatments on *N*-nitrosamine precursor concentrations.



## 1. INTRODUCTION

Drinking water sources impacted by wastewater treatment plant (WWTP) discharges contain natural organic matter (NOM) rich in organic nitrogen.<sup>1</sup> Chloramination, and to a lesser extent ozonation, chlorination, and chlorine dioxide disinfection,<sup>1</sup> of waters containing WWTP-derived NOM results in formation *N*-nitrosamines, a nonhalogenated group of disinfection byproducts (DBPs).<sup>2</sup> Despite their formation at low nanogram per liter levels, the high toxicity of *N*-nitrosamines has resulted in their consideration for regulation in drinking water.<sup>3</sup> The most commonly occurring *N*-nitrosamine in drinking waters is *N*-nitrosodimethylamine (NDMA), but studies by Mitch and colleagues have shown that NDMA may comprise only ~5% of total *N*-nitrosamines (TONO) in chloramine systems.<sup>4</sup>

Discovery of a spectroscopic surrogate for TONO precursors could be transformative for developing treatment processes to curb *N*-nitrosamines. Typically, TONO measurement requires 0.5–1.0 L samples<sup>5</sup> and takes a week or two to perform, which limits assessment of TONO precursor removal in lab-scale treatment processes. Similar to precursor surrogates for trihalomethanes (TTHMs)<sup>6</sup> and dihaloacetonitriles (DHANs),<sup>7</sup> a useful surrogate would consist of spectroscopic measurement(s) on waters prior to chloramination that

strongly correlate with the TONO formation potential (TONOFP). Preliminary work showed only moderate fluorescence-based correlations with TONOFP ( $R^2 < 0.50$ ),<sup>8</sup> but a recent study points to a possible improvement. Wang et al.<sup>9</sup> showed that the presence of humics led to underestimation of proteins (35–52%) because of fluorescence quenching. This is notable because protein-like fluorophores are a likely source of TONO precursors.<sup>2,8,10</sup>

To quantify the true (i.e., unquenched) proteins, Wang et al.<sup>9</sup> recommended separating the humic- and protein-like fractions by exploiting differences in their size distributions. As proteins have molecular weights higher than those of humics, size-based separation prior to fluorescence measurement could facilitate more accurate assessments of protein-like fluorophores. Asymmetric flow field-flow fractionation (AF4) is a flow-driven separation technology that has been used to measure NOM size distributions and requires no sample preconcentration and small sample volumes (~0.5 mL).<sup>11</sup> AF4 with inline

Received: April 22, 2017

Revised: May 10, 2017

Accepted: May 12, 2017

Published: May 12, 2017

Table 1. Sample Water Characteristics and Collection Details

sample name	date collected	disinfection method	pH	DOC (mg L <sup>-1</sup> )	SUVA (L mg <sup>-1</sup> m <sup>-1</sup> )	DON <sup>i</sup> (mg L <sup>-1</sup> )	TONOFP <sup>j</sup> (ng L <sup>-1</sup> )	TTHMFP <sup>k</sup> (μg L <sup>-1</sup> )	DHANFP <sup>l</sup> (μg L <sup>-1</sup> )
BRV_SEC <sup>a</sup>	4/13/16	UV	7.81	10.1	1.79	13.78	2640	73.2	20.6
BRV_FIN <sup>b</sup>	4/13/16	UV	7.69	12.3	1.54	16.59	359	87.3	20.2
BTN_SEC <sup>c</sup>	3/25/16	UV	7.53	5.4	1.86	3.07	973	37.3	10.4
BTN_FIN <sup>c</sup>	3/25/16	UV	7.85	5.5	1.79	2.82	1655	38.1	10.2
NACA_SEC <sup>d</sup>	3/31/16	UV	7.65	7.9	1.64	4.64	1603	58.1	15.7
NACA_FIN <sup>d</sup>	3/31/16	UV	7.69	7.8	1.60	6.28	2398	50.8	12.1
NLD_SEC <sup>e</sup>	3/18/16	ozone	7.82	9.6	1.30	2.85	1576	52.0	14.2
NLD_FIN <sup>e</sup>	3/18/16	ozone	7.73	8.1	0.78	2.87	241	33.1	3.4
RGS_SEC <sup>f</sup>	3/25/16	chlorine	7.44	6.6	1.70	3.45	1433	41.9	12.6
RGS_FIN <sup>f</sup>	3/25/16	chlorine	7.69	6.7	1.54	3.67	462	38.1	10.9
SPD_SEC <sup>g</sup>	3/25/16	chlorine	7.70	7.7	1.70	2.60	2414	49.8	14.8
SPD_FIN <sup>g</sup>	3/25/16	chlorine	7.64	7.5	1.57	2.47	1724	47.1	13.7
WS_SEC <sup>h</sup>	3/17/16	UV	7.40	5.2	1.63	3.41	963	30.3	8.2
WS_FIN <sup>h</sup>	3/17/16	UV	7.78	5.3	1.55	3.41	1016	29.3	8.0

<sup>a</sup>Berryville Waste Water Plant, Berryville, AR; secondary effluent (SEC). <sup>b</sup>Finished effluent (FIN). <sup>c</sup>Bentonville Wastewater Treatment Plant, Bentonville, AR. <sup>d</sup>Northwest Arkansas Conservation Authority Regional Treatment Facility, Bentonville, AR. <sup>e</sup>Noland Wastewater Treatment Facility, Fayetteville, AR. <sup>f</sup>Rogers Pollution Control, Rogers, AR. <sup>g</sup>Springdale Wastewater Treatment Plant, Springdale, AR. <sup>h</sup>West Side Wastewater Treatment Facility, Fayetteville, AR. <sup>i</sup>Dissolved organic nitrogen. <sup>j</sup>Total *N*-nitrosamine formation potential. <sup>k</sup>Total trihalomethane formation potential. <sup>l</sup>Dihaloacetonitrile formation potential.

fluorescence detection (FLD) can potentially characterize protein-like fluorophores following separation from interfering humics, but to the best of our knowledge, no studies have employed this technique to assess TONO precursors.

The objective of this study is to leverage AF4-based metrics of protein-like fluorophores to develop a TONO precursor surrogate. AF4-FLD fractograms were collected on WWTP effluents before and after oxidative treatments. Following chloramination of these samples, TONOFP was measured by chemiluminescence and correlations were sought using a single regression and multiple regressions. The resultant TONO precursor surrogate can be leveraged to assess the impact of oxidative treatments of *N*-nitrosamine precursor concentrations.

## 2. MATERIALS AND METHODS

**2.1. Sample Description and Water Quality Measurements.** Fourteen sample waters were collected from seven WWTPs, from each plant effluent (called finished effluent), and prior to the final disinfection process (called secondary effluent), which included UV, ozonation, and chlorination. Details regarding the sample waters are provided in Table 1. Sample waters were filtered with 0.45 μm poly(ether sulfone) (PES) membranes prerinsed with 500 mL of Milli-Q water and stored in low-density polyethylene carboys at 4 °C in the dark prior to use. Raw water characteristics were measured upon collection and are summarized in Tables 1, S1, and S2. Fluorescence excitation–emission matrices (EEMs) and water quality parameters were measured following the procedure described by Needham et al.,<sup>8</sup> with the exception of TDN, which is detailed in the Supporting Information. Dissolved organic nitrogen (DON) was calculated as the difference between TDN and inorganic nitrogen (Table 1).

**2.2. Experimental Procedures.** **2.2.1. DBPFP.** The DBP formation potential (DBPFP) was measured using the protocol developed by Do et al.,<sup>7</sup> which was modified from Standard Methods 5710-B and -D,<sup>8</sup> with a monochloramine dose of 250 mg L<sup>-1</sup> as Cl<sub>2</sub> at pH 7. TTHMFP and DHANFP were measured by gas chromatography with an electron capture

detector to test the assumption that the AF4-FLD metrics were most applicable to TONOFP. While formation potential tests at pH 7 may not maximize formation of NDMA,<sup>12</sup> it was selected to achieve quantifiable concentrations of TONO while not incurring base-catalyzed destruction of DHAN,<sup>13</sup> which would inhibit assessment of these precursors.<sup>7</sup> TONO analysis is preceded by solid phase extraction (SPE), modified from EPA Method 521, and adapted from Needham et al.<sup>8</sup> by acidifying samples to pH 2 using sulfamic acid.<sup>5</sup> An Eco Physics CLD 88sp chemiluminescence NO detector is used to quantify TONO, following the approach detailed by Mitch and Dai.<sup>14</sup> As some TONO can exist in WWTP samples prior to formation potential tests, TONO measurements were made on secondary and finished effluent samples prior to chloramination.

**2.2.2. AF4-FLD Fractograms.** AF4-FLD fractograms were collected with a Postnova Analytics AF2000-MT AF4 system with an inline dual-monochromator fluorescence detector (Agilent Technologies). A 0.01 mM phosphate buffer at pH 7 was used as the system eluent. The AF4 separation channel was backed with a 10 kDa regenerated cellulose membrane and had a length of 27.4 cm, and its width tapered from 2.0 cm near the inlet to 0.7 cm at the outlet. An autosampler was used to inject 0.5 mL of prefiltered sample water (0.45 μm PES) onto the membrane. The developed AF4 method utilizes a combination of slot flow and high cross-flow (Table S4). For the AF4 fractograms, fluorescence was measured at an excitation of 280 nm and a scan of emission wavelengths between 305 and 500 at 5 nm step sizes to target wavelengths associated with protein-like fluorophores.<sup>15</sup> The fluorescence intensity excitation and emission wavelengths chosen for fractograms were 280 and 340 nm, respectively (i.e., *I*<sub>280/340</sub>), to maximize the signal-to-noise ratio. Fractogram *x*-axes were converted from elution time to molecular weight using a standard curve generated from measurements of polystyrene sulfonate (PSS) standards with molecular weights ranging from 30 to 1000 kDa (Figure S1). The standard curve was applied to samples through an elution time of 25 min when the cross-flow undergoes a transition to zero, after which the molecular weight is no longer quantifiable. PSS standards with molecular weights of 2000 and 3200 kDa were also measured but did not elute

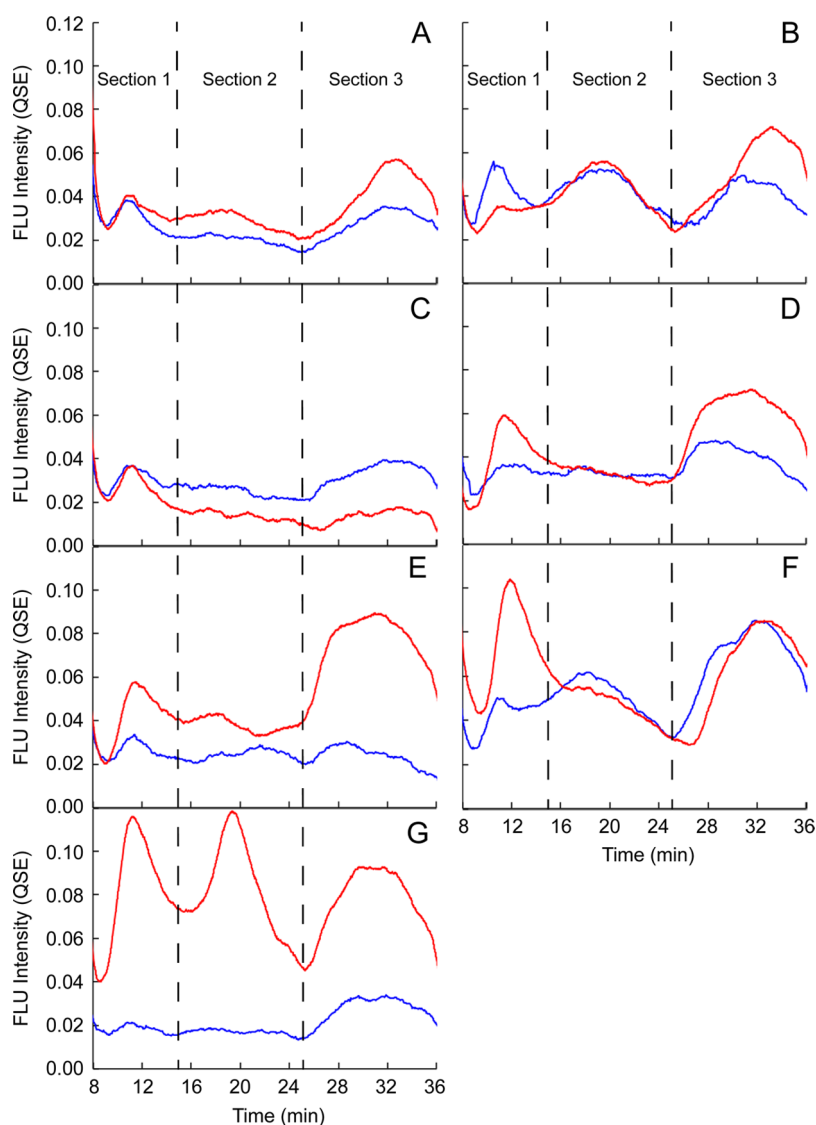


**Figure 1.** AF4-FLD fractograms ( $I_{280/340}$ ) for WWTP samples taken prior to the final disinfection stage, termed secondary effluent (red) and finished effluent (blue) samples. (A) BRV, (B) BTN, (C) NACA, and (D) WS WWTPs utilize UV disinfection; (E) RGS and (F) SPD use chlorine disinfection, and (G) NLD uses ozone disinfection. Dashed vertical lines indicate the times used to distinguish sections 1–3 and variables AUC1–AUC3.

until after the cross-flow ceased and were not incorporated into the standard curve. They do, however, illustrate that this nonquantifiable fraction is likely comprised of high-molecular weight compounds (i.e., >1500 kDa).

**2.3. AF4-FLD Processing.** AF4-FLD fractograms were analyzed to develop variables to be assessed as TONO precursor surrogates. Fractograms were divided into three sections beginning at an elution time of 8.50 min, which corresponds to the end of the void peak. Section 1 covers 8.50–14.88 min of elution time, with the latter corresponding to a local minimum calculated as the average of the elution times of the local minima of all fractograms. Section 2 covers 14.88–25 min, and section 3 is the unquantifiable peak from 25 min through the end of the run. The area under the curve (AUC) within the three sections was calculated as AUC1–AUC3. Additionally, the variable Max represents the maximal peak height in sections 1 and 2 taken together. Exploration of the maximal peak height in the individual sections is included in the [Supporting Information](#). An additional variable, Intensity,

was utilized that originated from the EEMs of the unfractionated samples. Specifically, the fluorescence intensity at all wavelengths pairs was correlated to TONOPF to determine the point of maximal  $R^2$ , which for TONO was  $I_{225/301}$ . However, the independent variable Intensity was chosen as  $I_{225/310}$  for TONO, which was the closest pair to  $I_{225/301}$  that fell within previously reported ranges for nitrosamine precursors.<sup>15</sup> This Intensity value was used to determine which multivariate models showed promise, as detailed in [section 2.4](#). After significant models had been identified, the models were recalculated with each of 57750 wavelength pairs measured in the EEMs to determine the best model. The wavelength pair corresponding to the best model is termed Intensity\*. Values of AUC1–AUC3, Max, Intensity, and Intensity\* for TONO are listed in [Table S5](#), and a discussion of Intensity and Intensity\* for TTHM and DHAN is included in the [Supporting Information](#).

**2.4. Model Development.** To assess correlations between TONOPF and AF4-FLD variables, several statistical models

were developed. Models were also developed to explore correlations with TTHMFP and DHANFP and are detailed in the Supporting Information. Simple linear regression models were developed between TONOFF and each of the AF4-FLD variables and DON. Multiple-regression models were formulated using combinations of AUC1–AUC3, Max, Intensity, and DON. For all models, independent variables were assumed to be non-zero and significant if their coefficients had  $p$  values of  $<0.05$ . All presented  $R^2$  values are adjusted for the number of independent variables to fairly compare models with differing numbers of variables.<sup>16</sup> Additionally, all model types were explored for their suitability to predict the impact of oxidative treatment (i.e., chlorination, ozonation, and UV treatment) on DBPFP. DBPFP ratios were generated as the formation potential of the finished effluent sample divided by that of the secondary effluent sample for each plant. These ratios indicate the change in DBP precursors caused by oxidative treatment ( $n = 7$ ). Similarly, ratios were calculated for the independent variables from AF4-FLD, fluorescence EEMs, and water quality parameters, which included AUC1–AUC3, Max, Intensity, and DON. For example, AUC1 ratio is the value of AUC1 for the finished effluent of a given WWTP divided by AUC1 of the secondary effluent sample from the same plant, as shown in Figure S2.

### 3. RESULTS AND DISCUSSION

**3.1. AF4-FLD.** Figure 1 shows AF4-FLD fractograms (at  $I_{280/340}$ ) for WWTP samples from the secondary effluent and finished effluent. The AF4-FLD fractograms had peaks at approximately 11, 20, and 31 min, although the locations of precise peak maxima varied among the samples. Using Figure S1, the first peak corresponds to 10–445 kDa, the second peak corresponds to 445–1500 kDa, and the final peak is unquantifiable but likely corresponds to a NOM of  $>1500$  kDa. For most of the WWTP samples, the intensity of these peaks decreased following disinfection, indicating partial oxidation or removal of these NOM fractions. However, in a few cases (i.e., section 1 in Figure 1B, sections 1–3 in Figure 1C, and section 2 in Figure 1F), peak heights increased following disinfection, possibly because of the physical breakdown of a larger NOM (i.e., oxidation of material in section 3 forming material in section 1). The impact of the oxidative treatments on TONOFF is explored in subsequent sections.

**3.2. Model Development.** Models were first generated for the entire data set of TONOFF values (Table 1). Neither simple linear nor multivariate models produced strong correlations between TONOFF and AF4-FLD metrics or DON, with the strongest linear correlation being to AUC1 (adjusted  $R^2 = 0.22$ ). A maximal adjusted  $R^2$  of 0.36 was obtained between TONOFF and Intensity ( $I_{225/310}$ ), which was not an improvement over similar models in ref 8.

Cursory comparison of TONOFF (Table 1) and AUC1 (Table S5) indicated three of the four WWTPs utilizing UV disinfection had TONOFF in finished effluent samples higher than that of the secondary effluent samples, two of which were mirrored by similar responses in AUC1. This indicates that UV disinfection can generate TONO precursors, similar to the findings of Dai et al.,<sup>17</sup> particularly in the presence of coagulant aid polymers.<sup>18</sup> The DON Ratio was not found to be significant in any multivariate models. While poor correlations were observed between TONOFF and AUC1 in models comparing these values directly, notable correlations emerge in models

between TONOFF Ratio (i.e., TONOFF of the finished effluent sample divided by that of the secondary effluent sample) and ratios of AF4-FLD metrics and Intensity (Figure 2). Intensity in the TONOFF Ratio models corresponds to

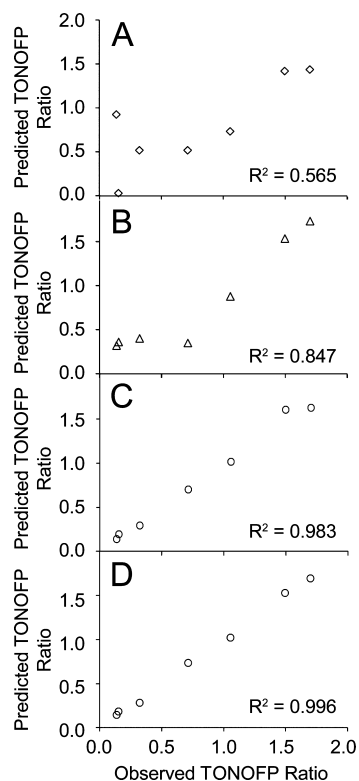


**Figure 2.** Multivariate models of (A) TONOFF Ratio with AUC1 Ratio, (B) AUC1 and Max Ratio, (C) AUC1, Max, and Intensity Ratio ( $I_{225/310}$ ), and (D) AUC1, Max, and Intensity\* Ratio ( $I_{257/277}$ ). Observed TONOFF Ratios were calculated for each WWTP as the TONOFF of the secondary effluent sample divided by that of the finished effluent sample. The model in panel A is  $\text{TONOFF Ratio} = 1.38 \times \text{AUC1 Ratio} - 0.23$ . The model in panel B is  $\text{TONOFF Ratio} = 3.97 \times \text{AUC1 Ratio} - 3.44 \times \text{Max Ratio} + 0.23$ . The model in panel C is  $\text{TONOFF Ratio} = 4.56 \times \text{AUC1 Ratio} - 5.04 \times \text{Max Ratio} + 0.75 \times \text{Intensity Ratio} - 0.01$ . The model in panel D is  $\text{TONOFF Ratio} = 4.12 \times \text{AUC1 Ratio} - 4.36 \times \text{Max Ratio} + 0.63 \times \text{Intensity* Ratio} - 0.09$ . All  $R^2$  values are adjusted for the number of independent variables.

$I_{225/310}$ , which falls in the region associated with protein-like fluorophores.<sup>15</sup> Simple linear regression between TONOFF Ratio and AUC1 Ratio yields an adjusted  $R^2$  of 0.565 (Figure 2A). A multivariate model for AUC1 Ratio and Max Ratio (Figure 2B) has an adjusted  $R^2$  of 0.847, and for AUC1, Max, and Intensity Ratio (Figure 2C), the adjusted  $R^2$  is 0.983. The  $p$  value of this model is 0.0008, indicating that the model is significant. A model of AUC1, Max, and Intensity Ratio was further refined using each of the 57750 available wavelength pairs in each EEM for Intensity Ratio. The best-fitting correlation coefficient corresponded to  $I_{257/277}$ , with an adjusted  $R^2$  value of 0.996 (Figure 2D). While this pair is outside the range typically reported for protein-like fluorophores, it is most closely adjacent to a subset of proteins, specifically tryptophan-like fluorophores.<sup>19</sup> The distribution of data indicates the model can predict TONOFF Ratios spanning from 0.136 to 1.701, encompassing both destruction and formation of TONO precursors from oxidative treatment. Another test of the

model's robustness was an inquiry into the influence of individual observations, which indicated no single observation held undue influence on the model as a whole and is discussed further in the [Supporting Information](#). In addition, as strong correlations were found only for models of TONOPF Ratio rather than discrete values of TONOPF, the model cannot be utilized to predict individual values of TONOPF but can be leveraged to predict the effect of oxidative treatment on TONO precursor concentrations.

To provide further insight into the nature of the precursor surrogate, TONO was measured on the WWTP samples prior to chloramination ([Table S3](#)). These data indicate background TONO was present at concentrations ranging from 89 to 192 ng L<sup>-1</sup> as NDMA, which comprised 7–54% of the TONO measured following the DBPFP tests. However, no significant models were generated excluding the background TONO (see details in the [Supporting Information](#)). This, coupled with the strength of the models in which TONOPF Ratios were calculated, including the background TONO ([Figure 2](#)), suggests that the independent variables in the model likely characterize the background TONO in addition to the protein-like TONO precursors that subsequently reacted with chloramines in the DBPFP tests. As such, it is likely that the background TONO affected the fluorescence-based metrics, a topic that should be studied systematically in future work.

The AF4-FLD method developed here is suitable for the separation and characterization of protein-like fluorophores in samples from WWTPs. Following transformation of the data to indicate changes produced by oxidative treatment, multivariate analysis revealed a strong size-resolved fluorescence-based TONO precursor surrogate. With an adjusted  $R^2$  of 0.996, a combination of AF4-FLD metrics (AUC1 and Max) and fluorescence EEMs ( $I_{257/277}$ ) can predict TONOPF Ratios across a wide range in which TONO precursors were both created and destroyed.

**3.3. Implications.** As the fluorescence metrics require just 2 mL of sample and can be acquired in less than 2 hours, this surrogate ([Figure 2D](#)) could be leveraged to assess the impact of oxidative treatment on *N*-nitrosamine precursor concentrations. Upcoming studies include evaluation of this surrogate to assess other TONO precursor removal processes (i.e., sorption) and characterization of the chemical moieties within the 10–445 and 445–1500 kDa peaks. The novel AF4-FLD method could provide insights into the nature of protein-rich NOM relevant to other areas of environmental science, including membrane fouling and biofilm soluble microbial products.

## ■ ASSOCIATED CONTENT

### 📄 Supporting Information

The Supporting Information is available free of charge on the [ACS Publications website](#) at DOI: [10.1021/acs.estlett.7b00147](https://doi.org/10.1021/acs.estlett.7b00147).

Lake water samples, dissolved organic nitrogen method and calculations, fractogram peak maxima, models of TTHMFP and DHANFP, influence of individual observations, TONOPF method development, and references ([PDF](#))

## ■ AUTHOR INFORMATION

### Corresponding Author

\*Department of Civil Engineering, University of Arkansas, 4190 Bell Engineering Center, Fayetteville, AR 72701. E-mail:

[julianf@uark.edu](mailto:julianf@uark.edu). Phone: (479) 575-4023. Fax: (479) 575-7168.

### ORCID

Julian L. Fairey: 0000-0003-3129-3929

### Notes

The authors declare no competing financial interest.

## ■ ACKNOWLEDGMENTS

Financial support from the National Science Foundation (Grant CBET #1254350 to J.L.F.) and a University of Arkansas Doctoral Academy Fellowship (to E.M.N.) is gratefully acknowledged. The authors acknowledge Erik Pollock of the University of Arkansas Stable Isotopes Lab for running the total nitrogen samples.

## ■ REFERENCES

- (1) Sirivedhin, T.; Gray, K. A. 2. Comparison of the disinfection by-product formation potentials between a wastewater effluent and surface waters. *Water Res.* **2005**, *39*, 1025–1036.
- (2) Krasner, S. W.; Mitch, W. A.; McCurry, D. L.; Hanigan, D.; Westerhoff, P. Formation, precursors, control, and occurrence of nitrosamines in drinking water: A review. *Water Res.* **2013**, *47*, 4433–4450.
- (3) Hrudey, S. E.; Charrois, J. W. A. *Disinfection by-products and human health*; IWA Publishing and Australian Water Association: London, 2012; p 304.
- (4) Dai, N.; Mitch, W. A. Relative importance of *N*-nitrosodimethylamine compared to total *N*-nitrosamines in drinking waters. *Environ. Sci. Technol.* **2013**, *47*, 3648–3656.
- (5) Dai, N.; Shah, A. D.; Hu, L. H.; Plewa, M. J.; McKague, B.; Mitch, W. A. Measurement of Nitrosamine and Nitramine Formation from NO Reactions with Amines during Amine-Based Carbon Dioxide Capture for Postcombustion Carbon Sequestration. *Environ. Sci. Technol.* **2012**, *46*, 9793–9801.
- (6) Pifer, A. D.; Fairey, J. L. Improving on SUVA<sub>254</sub> using fluorescence-PARAFAC analysis and asymmetric flow-field flow fractionation for assessing disinfection byproduct formation and control. *Water Res.* **2012**, *46*, 2927–2936.
- (7) Do, T. D.; Chimka, J. R.; Fairey, J. L. Improved (and singular) disinfectant protocol for indirectly assessing organic precursor concentrations of trihalomethanes and dihaloacetonitriles. *Environ. Sci. Technol.* **2015**, *49*, 9858–9865.
- (8) Needham, E. M.; Sidney, S. M.; Chimka, J. R.; Fairey, J. L. Trihalomethane, dihaloacetonitrile, and total *N*-nitrosamine precursor adsorption by carbon nanotubes: the importance of surface oxides and pore volume. *Environ. Sci.: Water Res. Technol.* **2016**, *2*, 1004–1013.
- (9) Wang, Z. G.; Cao, J.; Meng, F. G. Interactions between protein-like and humic-like components in dissolved organic matter revealed by fluorescence quenching. *Water Res.* **2015**, *68*, 404–413.
- (10) Liao, X. B.; Wang, C. K.; Wang, J.; Zhang, X. J.; Chen, C.; Krasner, S. W.; Suffet, I. H. Nitrosamine precursor and DOM control in effluent-affected drinking water. *J.—Am. Water Works Assoc.* **2014**, *106*, E307–E318.
- (11) Pifer, A. D.; Miskin, D. R.; Cousins, S. L.; Fairey, J. L. Coupling asymmetric flow-field flow fractionation and fluorescence parallel factor analysis reveals stratification of dissolved organic matter in a drinking water reservoir. *Journal of Chromatography A* **2011**, *1218*, 4167–4178.
- (12) Schreiber, I. M.; Mitch, W. A. Nitrosamine formation pathway revisited: The importance of chloramine speciation and dissolved oxygen. *Environ. Sci. Technol.* **2006**, *40*, 6007–6014.
- (13) Hua, G. H.; Reckhow, D. A. Evaluation of bromine substitution factors of DBPs during chlorination and chloramination. *Water Res.* **2012**, *46*, 4208–4216.
- (14) Mitch, W. A.; Dai, N. Development and application of a total nitrosamine assay for disinfected waters. Water Research Foundation Report 4209; Water Research Foundation: Denver, 2012; pp 49–51.

- (15) Hudson, N.; Baker, A.; Reynolds, D. Fluorescence analysis of dissolved organic matter in natural, waste and polluted waters - A review. *River Research and Applications* **2007**, *23*, 631–649.
- (16) Montgomery, D. C. *Applied Statistics and Probability for Engineers*, 6th ed.; John Wiley & Sons: Hoboken, NJ, 2013.
- (17) Dai, N.; Zeng, T.; Mitch, W. A. Predicting N-Nitrosamines: N-Nitrosodiethanolamine as a Significant Component of Total N-Nitrosamines in Recycled Wastewater. *Environ. Sci. Technol. Lett.* **2015**, *2*, 54–58.
- (18) McCurry, D. L.; Krasner, S. W.; von Gunten, U.; Mitch, W. A. Determinants of disinfectant pretreatment efficacy for nitrosamine control in chloraminated drinking water. *Water Res.* **2015**, *84*, 161–170.
- (19) Coble, P. G. Characterization of marine and terrestrial DOM in seawater using excitation emission matrix spectroscopy. *Mar. Chem.* **1996**, *51*, 325–346.